Modelling of a two-phase vortex-ring flow using an analytical solution for the carrier phase

O. Rybdylova[a,*], S.S. Sazhin[a], A.N. Osiptsov[b,a], F.B. Kaplanski[c,a], S. Begg[a], M. Heikal[a]

[a] *Sir Harry Ricardo Laboratories, Advanced Engineering Centre, School of Computing, Engineering and Mathematics, University of Brighton, Brighton BN2 4GJ, UK*
[b] *Laboratory of Multiphase Flows, Institute of Mechanics, Lomonosov Moscow State University, Moscow 119192, Russia*
[c] *Tallinn University of Technology, Akad. tee 15A, Tallinn 12618, Estonia*

Abstract

A transient axially symmetric two-phase vortex-ring flow is investigated using the one-way coupled, two-fluid approach. The carrier phase parameters are calculated using the approximate analytical solution suggested by Kaplanski and Rudi (Phys. Fluids vol. 17 (2005) 087101-087107). Due to the vortical nature of the flow, the mixing of inertial admixture can be accompanied by crossing particle trajectories. The admixture parameters are calculated using the Fully Lagrangian Approach (FLA). According to FLA, all of the dispersed phase parameters, including the particle/droplet concentration, are calculated from the solution to the system of ordinary differential equations along chosen particle trajectories; FLA provides high-accuracy particle number calculations even in the case of crossing particle trajectories (multi-valued fields of the dispersed media). Two flow regimes corresponding to two different initial conditions are investigated: (i) injection of a two-phase jet; and (ii) propagation of a vortex ring through a cloud of particles. It was shown that the dispersed media may form folds and caustics in these flows. In both cases, the ranges of governing parameters leading to the formation of mushroom-like clouds of particles are identified. The caps of the mushrooms contain caustics or edges of folds of the dispersed media, which correspond to particle accumulation zones.

*Corresponding author
Email address: O.Rybdylova@brighton.ac.uk (O. Rybdylova)

Keywords: Vortex Ring, Dusty Gas, Two-phase flow, Fully Lagrangian approach
PACS: 47.32.C-, 47.55.Kf
2010 MSC: 76T10

1. Introduction

Two-phase vortex-ring flows are widely observed in engineering and environmental conditions [1, 2], including direct injection internal combustion engines [3]. In such flows, the admixture forms high concentration regions with folds (local zones of crossing particle/droplet trajectories, hereafter referred to as particles) and caustics. The Eulerian approaches cannot describe such regions with reasonable accuracy, since these approaches are based on the assumption of single-valued fields of the particle concentration and velocities. Ferry and Balachandar [4] showed that the condition for uniqueness of the particle velocity field is related to the particle response time and the maximal compressional strain of the dispersed phase flow. This uniqueness was shown to be expected for small compressional strains, and short particle response times, which correspond to small particle Stokes numbers. As shown by Healy and Young [5], the only method capable of calculating the particle concentration field in the case of multi-valued admixture parameter fields, without using excessive computer power, is the one suggested by Osiptsov [6], known as the Fully Lagrangian Approach (FLA). At the edge of a local region of crossing particle trajectories (caustics), the particle number density has a singularity. This is a well-known feature of the mathematical model of the collisionless continuum of point particles (see details in [7]). In the latter paper, typical examples of flows with singularities in the particle number density field were analysed. It was shown that for an integrable singularity of particle number density, at the singular points the mean distance between the particles remains finite and the model of collisionless particles remains valid. Our study is focused on further investigation of these types of flows based on the previously developed vortex ring models for the carrier phase and the Fully Lagrangian Approach (FLA) for the dispersed phase. Particular attention is paid to the details of the mixing process with regions of high particle concentration, which can potentially lead to the formation of unfavourable zones of high fuel vapour concentration in internal combustion engines, when particles are identified with fuel droplets.

Vortex-ring flows have been extensively studied theoretically and experimentally [1, 2, 8, 9, 10, 11, 12, 13, 14]. Theoretical studies have been mainly focused on vortex rings in the limits of high [10, 11] and low [15, 16] Reynolds numbers based on the initial velocity circulation and the ring radius (see [17] for an overview of vortex ring propagation models). In [18], the analytical solution suggested by Kaplanski and Rudi [19] was applied to the analysis of particle dynamics and mixing in an oscillating vortex pair, using the conventional Lagrangian approach. An alternative approach to simulation of the dynamics of particles in a 2D vortex pair formed by a plane jet, using the Fully Lagrangian Approach (but not the Kaplanski-Rudi solution) is described in [20].

Investigation of particle-laden vortex-ring flows is also important in studies of inertial-particle accumulation in turbulent flows. Yang and Shy [21] investigated particle distribution in turbulent flows experimentally, while Squires and Eaton [22], Goto and Vassilicos [23], Chen et al. [24], and Soldati and Marchioli [25] addressed it theoretically. These studies show that admixture distribution in turbulent flows crucially depends on the vortex structures. In the cases where the density of the particle material is higher than the density of the carrier phase, accumulation zones were shown to be formed on the edges of intense local vortices. These findings agree with the results of experimental and theoretical studies of the interactions of particles with vortex structures [26, 27, 28]. Foster, Duck, and Hewitt [27] studied particle concentrations in the framework of the Eulerian approach. Soldati and Marchioli [25] used Lagrangian tracking together with statistical tools in order to quantify particle segregation. Lebedeva and Osiptsov[28] used FLA to calculate particle number density fields in a steady-state, axially symmetric, tornado-like flow.

In the present study, a two-phase vortex-ring flow is considered in the framework of the two-fluid (inter-penetrating continua) approach [29]. According to this approach, a cloud of particles is described using continuum values of velocity and number density of the dispersed media. In contrast to previous studies, the approach used in our paper is based on the Kaplanski-Rudi [19] analytical solution for the carrier phase and the Fully Lagrangian Approach for the dispersed phase. The choice of such a combined (analytical and numerical) approach is supported by the fact that in the flow considered, the mixing process can be accompanied by crossing particle trajectories, the onset of local zones of multi-valued particle parameters, caustics and particle accumulation regions. The analytical solution for the carrier phase and the

use of FLA for the dispersed phase allows us to calculate particle number density correctly with high accuracy. Our analysis is focused on an axially symmetric vortex ring rather than a plain vortex pair flow considered earlier in [28]. The Kaplanski-Rudi [19] analytical model was compared against DNS simulations in [13]. Analytical and numerical models showed good agreement. However, it is not clear if the combination of the analytical solution based on the self-similar variables with FLA could be applicable to simulate two-phase vortex ring flows.

The mathematical model of the two-phase vortex ring flow, used in the analysis, and mathematical formalism of the Kaplanski-Rudi model are discussed in Section 2. In Section 3, two-phase jet injection and the propagation of a vortex ring through a cloud of dust are considered. The main results of the paper are summarised in Section 4.

2. Formulation of the problem

We consider an axially symmetric transient flow of a two-phase gas-particle mixture, interacting with a vortex ring, and introduce a cylindrical coordinate system as shown in Fig. 1. The vortex ring propagates along the z-axis (the axis of symmetry); at the initial instant of time the vortex ring is assumed to be confined by the $z = 0$ plane, R_0 is the initial vortex ring radius.

The problem is studied in the framework of the one-way coupled, two-fluid approach [29]. The carrier phase is an incompressible viscous gas, described by the Navier-Stokes equations. The particles are assumed to be spheres of identical radii and masses, treated as a pressureless continuum; the particle mass loading is assumed to be small and the effects of the admixture on the carrier phase are ignored. We took into account the effects of the gravity force and the aerodynamic drag approximated by the corrected Stokes drag force [30]. The correction takes into account the effect of finite Reynolds numbers of the flow around a particle (Re_d). The expression for the total force acting on a particle is presented as [30]:

$$\mathbf{f} = 6\pi\sigma^*\mu\left(\mathbf{v}^* - \mathbf{v}_d^*\right)\chi_d + m\mathbf{g}, \tag{1}$$

where $\chi_d = 1 + \mathrm{Re}_d^{2/3}/6$, $\mathrm{Re}_d = 2\rho\sigma^*\left|\mathbf{v}^* - \mathbf{v}_d^*\right|/\mu$, $\mathbf{g}$ is the acceleration due to gravity; the asterisk indicates the dimensional parameters; subscript '$_d$' refers to the dispersed phase, ρ and μ are the gas density and dynamic viscosity, respectively; σ^* is the particle radius.

The following non-dimensional parameters are introduced:

$$\mathbf{r}_{(d)} = \frac{\mathbf{r}^*_{(d)}}{R_0},\ \mathbf{v}_{(d)} = \frac{R_0}{\Gamma_0}\mathbf{v}^*_{(d)},\ t = \frac{\Gamma_0}{R_0^2}t^*,\ n_d = \frac{n_d^*}{n_{d0}}, \tag{2}$$

where the carrier phase (parameters without subscript) and the dispersed phase (with subscript '$_d$') coordinates and velocities are normalised using the same length and velocity scales; $\mathbf{r} = (r, z)$, $\mathbf{r}_d = (r_d, z_d)$, $\mathbf{v} = (u, v)$, $\mathbf{v}_d = (u_d, v_d)$, Γ_0 is the initial circulation of the vortex ring, n_{d0} – characteristic value of the initial number density.

Kaltaev [15] obtained an analytical solution to the vorticity equation corresponding to the Stokes flow ($\mathrm{Re} = \rho\Gamma_0/\mu = 0$) for the case, when at the initial instant of time the vorticity distribution is set as $\zeta = \delta(z)\,\delta(r-1)$ (see also [31]). In the reference frame fitted to the vortex ring, this solution can be presented as:

$$\zeta = \frac{1}{4\sqrt{\pi}}t^{-3/2}\exp\left(-\frac{z^2+r^2+1}{4t}\right)\mathrm{I}_1\left(\frac{r}{2t}\right),$$

where I_1 is the modified Bessel function.

Since the governing Stokes equation is linear, the expression for the vorticity distribution in the stationary frame of reference can be rewritten as:

$$\zeta = \frac{1}{4\sqrt{\pi}}t^{-3/2}\exp\left(-\frac{(z-z_{vc})^2+r^2+1}{4t}\right)\mathrm{I}_1\left(\frac{r}{2t}\right), \tag{3}$$

where $z_{vc} = z_{vc}(t)$ is the position of the vortex centroid.

Kaplanski-Rudi [19] suggested to generalise Solution (3) to the case of small but finite Reynolds numbers based on the initial velocity circulation and the ring radius and rewrite it as (cf. [32]):

$$\zeta = \frac{\mathrm{Re}^{3/2}}{4\sqrt{\pi}}t^{-3/2}\exp\left(-\mathrm{Re}\frac{(z-z_{vc})^2+r^2+1}{4t}\right)\mathrm{I}_1\left(\mathrm{Re}\frac{r}{2t}\right). \tag{4}$$

Solution (4) can be derived from Equation (3) by rescaling time $\tilde{t} = t/\mathrm{Re}$, $\mathrm{Re} = \rho\Gamma_0/\mu$. This solution was studied in a number of papers, e.g. [16, 19, 32] to name a few. Kaplanski and Rudi [33] show that Solution (4) becomes a Gaussian distribution of vorticity and Phillips self-similar solution in the limits of $\sqrt{\tilde{t}} = \sqrt{t/\mathrm{Re}} \to 0$ and $\sqrt{\tilde{t}} = \sqrt{t/\mathrm{Re}} \to \infty$, respectively. These

correspond to the initial stage of a vortex ring development and its decay stage, respectively.

In this case, the expressions for the stream function (Ψ) and the translational velocity (V_{vc}) were presented as [19]:

$$\Psi = -\frac{r\sqrt{\mathrm{Re}}}{4\sqrt{2t}} \int_0^\infty F\left(x, \sqrt{\mathrm{Re}}\frac{z-z_{vc}}{\sqrt{2t}}\right) \mathrm{J}_1\left(\sqrt{\mathrm{Re}}\frac{x}{\sqrt{2t}}\right) \mathrm{J}_1\left(\sqrt{\mathrm{Re}}\frac{rx}{\sqrt{2t}}\right) dx, \quad (5)$$

$$F(x,y) = \exp(xy)\,\mathrm{erfc}\left(\frac{x+y}{\sqrt{2}}\right) + \exp(-xy)\,\mathrm{erfc}\left(\frac{x-y}{\sqrt{2}}\right);$$

$$V_{vc} = \frac{\sqrt{\mathrm{Re}}}{4\sqrt{2t}} t^{-1/2} \left[3\exp\left(-\frac{\mathrm{Re}}{4t}\right)\mathrm{I}_1\left(\frac{\mathrm{Re}}{4t}\right) + \frac{\mathrm{Re}}{24t}\,{}_2F_2\left(\left\{\frac{3}{2},\frac{3}{2}\right\},\left\{\frac{5}{2},3\right\},-\frac{\mathrm{Re}}{2t}\right) - \right.$$
$$\left. -\frac{3\mathrm{Re}}{10t}\,{}_2F_2\left(\left\{\frac{3}{2},\frac{5}{2}\right\},\left\{2,\frac{7}{2}\right\},-\frac{\mathrm{Re}}{2t}\right)\right], \quad (6)$$

where J_1 is the Bessel function of the first kind, ${}_2F_2$ is the generalised hypergeometric function.

The vortex ring translational velocity (6) was shown to be in good agreement with the results obtained for high and low Reynolds numbers of the flow based on the initial velocity circulation and the ring radius in the limiting cases $t \to 0$ and $t \to \infty$ [16].

Solution (5) is not a rigorous solution to the nonlinear NavierStokes equation. However, in a number of papers, including [16, 34, 35], it was shown that the integral characteristics based on this solution, such as translational velocity V_{vc} and energy, are very weak functions of the Reynolds number for all times. The predictions of the Kaplanski and Rudi model were verified against the predictions of direct numerical simulations (DNS) and demonstrated satisfactory accuracy (see [34] for the details).

In the present study, we use Solutions (5) and (6) in order to obtain a qualitative description of two-phase vortex-ring flow in the case of finite Reynolds numbers based on the initial velocity circulation and the ring radius.

The dispersed phase is modelled using the Fully Lagrangian Approach [6], which makes it possible to calculate all of the dispersed phase parameters

including number density, from the solutions to the systems of ordinary differential equations along chosen particle trajectories:

$$n_d r_d \left|J\right| = n_{d0} r_{d0} \tag{7}$$

$$\frac{\partial \mathbf{r}_d}{\partial t} = \mathbf{v}_d, \quad \frac{\partial \mathbf{v}_d}{\partial t} = \frac{1}{\mathrm{Stk}}(\mathbf{v} - \mathbf{v}_d)\chi_d + \frac{1}{\mathrm{Fr}^2}\mathbf{e}_z, \tag{8}$$

$$\frac{\partial J_{ij}}{\partial t} = q_{ij}, \tag{9}$$

$$\frac{\partial q_{ij}}{\partial t} = \frac{1}{\mathrm{Stk}}\left(\frac{\partial v_i}{\partial r}J_{rj} + \frac{\partial v_i}{\partial z}J_{zj} - q_{ij}\right)\chi_d + \frac{1}{\mathrm{Stk}}\left(v_i - v_{di}\right)\frac{\partial \chi_d}{\partial x_{j0}}, \tag{10}$$

$$\frac{\partial \chi_d}{\partial x_{j0}} = \frac{1}{9}\frac{\mathrm{Re}_{d0}}{\mathrm{Re}_d^{1/3}}\frac{1}{|\mathbf{v} - \mathbf{v}_d|}\left(\left(u - u_d\right)\left(\frac{\partial u}{\partial r}J_{rj} + \frac{\partial u}{\partial z}J_{zj} - q_{rj}\right) + \right.$$
$$\left. + \left(v - v_d\right)\left(\frac{\partial v}{\partial r}J_{rj} + \frac{\partial v}{\partial z}J_{zj} - q_{zj}\right)\right),$$

where

$$J_{ij} = \frac{\partial x_i}{\partial x_{j0}}, \quad q_{ij} = \frac{\partial v_{di}}{\partial x_{j0}},$$

$$\mathrm{Stk} = \frac{m\Gamma_0}{6\pi\sigma\mu R_0^2}, \quad \mathrm{Fr} = \frac{\Gamma_0}{R_0\sqrt{gR_0}}, \quad \mathrm{Re}_d = \mathrm{Re}_{d0}\left|\mathbf{v} - \mathbf{v}_d\right|, \quad \mathrm{Re}_{d0} = \frac{2\sigma\Gamma_0}{R_0\nu},$$

indices i and j take values of r or z; $\mathbf{e}_z$ is the unit vector along the z-axis; r_{d0}, z_{d0} are the Lagrangian variables (the coordinates of initial particle positions); rJ is the Jacobian of the transform from the Eulerian to the Lagrangian coordinates. (7) is the continuity equation rewritten in the Lagrangian variables; (8) are momentum balance equations along chosen particle trajectories; (9) and (10) are additional equations to calculate the Jacobian components, they are derived from (8) by differentiation with respect to r_{d0} and z_{d0}. The initial conditions are presented as:

$$\begin{aligned} &r_d = r_{d0}, \quad z_d = z_{d0}, \\ &u_d = u_{d0}, \quad v_d = v_{d0}, \quad n_d = 1, \\ &q_{ij} = 0, \quad J_{ij} = \delta_{ij}, \end{aligned} \tag{11}$$

where δ_{ij} is Kronecker delta. The expressions for the velocity components and their derivatives follow from (5).

3. Results of numerical simulation

As mentioned above, Solution (5) and its analogue in the limiting case when $\mathrm{Re} \to 0$ were studied in [15, 19, 32]. Typical time evolutions of the vortex ring velocity and the position of the vortex centroid (z_{vc}) are shown in Fig. 2, $\mathrm{Re} = 100$. The position of the vortex centroid is calculated based on integrating Expression (6):

$$V_{vc} = \frac{dz_{vc}}{dt}, \quad z_{vc}\,(0) = 0, \tag{12}$$

(z-component) and from the solution of the equation $\partial\zeta/\partial r = 0$ (r-component). The latter equation can be rewritten as

$$\frac{\mathrm{Re}\, r_{vc}^2 + 2t}{\mathrm{Re}\, r_{vc}} = \frac{\mathrm{I}_0\,(0.5\mathrm{Re}\, r_{vc}/t)}{\mathrm{I}_1\,(0.5\mathrm{Re}\, r_{vc}/t)}. \tag{13}$$

At the initial stage, the vortex ring propagates with higher velocity and it's radius is almost constant. For the case of $\mathrm{Re} = 100$ (see Fig. 2), the decay of the vortex ring begins at $t \approx 75$, and is characterised by low vortex ring propagation velocity and slow growth of the vortex ring radius. This is consistent with the analysis of Solution (4) at the limits of $\sqrt{\tilde{t}} = \sqrt{t/\mathrm{Re}} \to 0$ and $\sqrt{\tilde{t}} = \sqrt{t/\mathrm{Re}} \to \infty$ (see Section 2).

We considered two problem formulations of the two-phase flow corresponding to two initial conditions. The first problem is the injection of a two-phase jet into a vortex ring. The second problem is the vortex ring propagation through a cloud of particles. Since Solution (5) has a singularity at $t = 0$, the initial time instant was taken as $t = t_0 > 0$. It was assumed that $\mathrm{Re} = 100$. 'Gas-particle' systems with two types of particles were considered: particles with lower inertia ($\mathrm{Stk} = 0.32, \mathrm{Re}_{d0} = 1$) and higher inertia ($\mathrm{Stk} = 8, \mathrm{Re}_{d0} = 5$) (see Table 1 for gasoline droplets and air mixture; $\mathrm{Re} = 100$; gasoline is approximated by a single-component fuel, iso-octane). System (7)–(10) of ordinary differential equations with initial conditions (11) was solved using the 4-th order Runge-Kutta method [36] for 441 and 861 chosen particle trajectories, for the case of jet injection and interation of a cloud of particles with the vortex ring respectively. In System (7)–(10), the values of the carrier phase velocity components and their derivatives (improper integrals) were calculated numerically.

The clouds of particles are subjected to significant deformations, leading to the formation of regions with high values of number density. The regions

σ^*, μm	Stk	Re_{d0}
50	8	5
10	0.32	1

Table 1: The droplet Stokes and Reynolds numbers.

of singularity of the particle number density are formed at the edges of the folds of the dispersed phase concentration field.

3.1. Two-phase jet injection with formation of a vortex ring

In order to simulate two-phase injection using Solution (5) and System (7)–(10) with initial conditions (11), various initial conditions for the dispersed phase were considered. It was found that two-phase vortex rings (mushroom-like clouds of particles) are formed if at initial time instant t_0 the $z-$component of particle velocity is set greater than that of the carrier phase. The results are presented in Figs. 3 and 4 for the following initial conditions:

$$\begin{aligned} &t_0 = 0.01, \quad r_d = r_{d0}, \quad z_d = z_{d0}, \\ &u_d = 5u\left(0, z_{vc}\left(t_0\right), t_0\right), \quad v_d = 0, \quad n_d = 1, \\ &q_{ij} = 0, \quad J_{ij} = \delta_{ij}. \end{aligned} \tag{14}$$

The highest degree of shading corresponds to the highest value of particle number density.

The two-phase flows with two particle sizes were considered. The cloud of particles with higher inertia propagates with higher velocity; it is subjected to smaller deformations and lesser number density variations. For example, in the case of Stk = 8, the number density is almost uniform: its variation is within 10%, with higher values in the core and lower values at the periphery of the jet (see Fig. 3). In the case of smaller particles, the cloud of particles takes a mushroom-like form. In the case of Stk = 0.32 (Fig. 4), the particle number density in the stalk of the mushroom is approximately 1; the highest particle concentration is observed in the cap region, where the particle number density reaches its maximum but finite value of 43 (the values of n_d were capped at 4 in Figs. 3–5 to improve visualisation of the results). The number density values are higher towards the periphery of the cap. In both cases, the clouds of particles overtook the vortex centroid and moved ahead of it. The effect of gravity leads to a positional shift of the cloud without affecting its shape;

their number densities remain the same as in the case when gravity was ignored.

Note that in both cases shown in Figs. 3 and 4, one can clearly see that the locations of the vortex ring-like structures identified by means of the particle number density fields are rather different from the locations of the vortex rings formed in the carrier phase. Thus the location of the carrier phase vortex rings cannot be identified based on the analyses of particle number densities in the general case. Thus, the reliability of the results of our previous analyses (e.g. [3]), where the location of the regions of maximal vorticity of the vortex ring-like structures in gasoline engines was identified based on the analysis of the particle velocities, can be questioned.

To investigate the effect of non-homogeneous initial distribution of particle number density, we assume that:

$$n_d(r, z, 0) = \frac{1}{1 + \exp(10(r - 0.9))} \tag{15}$$

The number density fields predicted for the cases of homogeneous and inhomogeneous initial distributions are compared in Fig. 5. As it can be seen from the figure, initial inhomogeneity of particle number density distribution leads to non-uniform distribution of this number density with radius along the centreline of the jet. The highest particle number density is observed in the periphery of the cap, similarly to the case of uniform initial number density distribution. The values of the number density are close in both cases.

The effect of particle inertia was studied for $0.02 \leq \sqrt{\rho/\rho_d} \leq 0.04$ (subscript $_d$ refers to dispersed phase (particles)), and $0.01 \leq \mathrm{Stk} \leq 100$, which corresponds to particles of various densities and sizes from a few to a few hundred micrometers. As follows from Figures 3-5 (and a number of similar figures not shown in the paper), the shape of the jet only slightly depends on the particle density. The effect of particle density is the most pronounced for $\mathrm{Stk} \sim 1 - 10$. In the case of large particles ($\mathrm{Stk} \sim 10 - 100$), the cloud of particles travels almost without deformation (see Fig. 4). The two-phase region turned out to be the broadest for $\mathrm{Stk} \sim 1$. The particles in the front of the jet interact with the vortex and form a wide cap. Particles behind the cap shift towards the axis and form a stalk of the mushroom-like two-phase jet. The tail of the cloud is extended along the centerline, stretching the cloud up to 10 times compared with the original cloud. The particle number density remains around 1 in the tail and reaches its highest value in the

mushroom cap. In the case of small particles, Stk ~ 0.01, the admixture velocity relaxes to the carrier phase velocity while particles remain inside the vortex ring. Therefore, the particles in this case move towards the centerline and stay behind the vortex ring; as the two-phase region stretches along the centreline, admixture number density decreases.

3.2. Propagation of a vortex ring in a dusty gas

The second problem considered is the propagation of a vortex ring through a cloud of particles. As in the first problem, the interactions of the vortex ring with particles of high and low inertia were considered. The initial conditions are assumed to be the following:

$$\begin{aligned} &t_0 = 0.2, \quad r_d = r_{d0}, \quad z_d = z_{d0}, \\ &u_d = 0, \quad v_d = 0, \quad n_d = 1, \\ &q_{ij} = 0, \quad J_{ij} = \delta_{ij}. \end{aligned} \tag{16}$$

The results of our numerical simulation are presented in Figs. 6–8. In the case of high-inertia particles (see Figs. 6 and 7), the initially rectangular-shaped cloud of particles deforms into a mushroom-like structure. The particles initially located at the periphery move towards the centerline, forming a stalk. The particles initially positioned closer to the axis of symmetry and closer to the vortex ring are pushed to the periphery. The cloud of particles turns inside out, so that the dispersed phase forms a fold. The time evolution of a Lagrangian frame formed by the dispersed particles in interaction with the vortex ring is shown in Fig. 7. The particle number density forms a singularity at the edge of the fold (see Fig. 7). The unbounded growth of particle number density on the edges of local regions of crossing particle trajectories (caustics) is a well known feature of the mathematical model of the collisionless continuum of point particles. The FLA allows us to simulate two-phase flows in the case of multi-valued particle parameter fields (folds) and to correctly calculate particle concentration at the edges of the fold. Note that this singularity of the particle concentration field is integrable and the assumption of the collisionless flow of particles remains valid when the particle volume fraction is sufficiently small. As shown in [7], for initial/characteristic particle volume fractions below 10^{-5} the interparticle collisions can be neglected even at the points of integrable singularities of n_d (see [7] for further details). Number densities higher than 4 are assumed to be equal to 4 in Figs. 7 and 8 to improve visualisation of the results. In the case of low-inertia particles

(see Fig. 8), the particles initially positioned closer to the axis of symmetry are accumulated near a 2D surface. Thus the originally rectangular-shaped cloud of particles deforms into a mushroom-like structure, similarly to the case considered earlier. The regions with the highest particle number density are formed at the cap sides.

As mentioned above, the particle number density increases without bound on the caustics (edges of the folds of the particle concentration field). Thus, one can expect that, with an increase in the initial volume fraction of the admixture, particle interactions may become possible in these regions. These, however, are not taken into account within the framework of FLA.

As in the cases shown in Figs. 3 and 4, one can clearly see in Figs. 7 and 8 that the locations of vortex ring-like structures identified based on the particle number densities are rather different from the locations of vortex rings formed in the carrier phase.

The interaction of a cloud of particles with vortex rings and particle transport in a vortex-ring flow take place in many environmental flows (flow of sediment particles in rivers, transport of sand, dust, pollutants in the air, distribution of plankton). The results presented in our paper agree qualitatively with the 2D simulation of a plane vortex pair propagating in a cloud of particles presented in [20] and with the experimental study of particle transport in a vortex ring [26]. In the latter papers it was observed that heavy particles are pushed away from the regions with high vorticity and accumulate near the edges of the vortex pair.

The Reynolds number for the fluid flow is based on the initial velocity circulation and describes the intensity of the vortex ring. A flow with higher or lower Reynolds number corresponds to a vortex ring with higher or lower intensity and higher/lower translational velocity. The velocity scale of the flow is related to the initial circulation and therefore the particle Stokes number is also related to the vortex ring intensity. The behaviour of the high and low inertia particles qualitatively remains the same, taking into account the scaling of the particle Stokes number.

4. Conclusion

Using the Fully Lagrangian Approach (FLA) for the dispersed phase and the Kaplanski-Rudi [19] analytical solution for the carrier phase, an axially symmetric transient particle-laden flow in a vortex ring has been investigated.

The FLA is believed to be the only approach to be able to correctly predict the particle concentration field in the flow with crossing particle trajectories.

It was shown that the Kaplanski-Rudi [19] analytical solution may be used to simulate both injection of a two-phase jet with a vortex ring field and interaction of a vortex ring with a cloud of particles if the particle inertia parameter Stk $\sim 0.1 - 10$. In both cases, the flow regimes leading to the formation of the two-phase mushroom-shaped structures with distinct zones of particle accumulation are predicted. For both problem formulations, it was shown that the two-phase ring-like structure position differs from the vortex ring of the carrier phase. This is attributed to the admixture inertia. In the case when particles are identified with fuel droplets directly injected into a combustion chamber, these zones of particle accumulation are expected to lead to the unfavourable formation of zones of rich fuel vapour concentration. It has been observed that in some cases, the dispersed medium forms folds and caustics with singularities and local zones of particle accumulation in the concentration fields. Accurate calculations of number density in these zones could not be performed if the analysis was based on the conventional rather than the Fully Lagrangian Approach.

Acknowledgements

The authors are grateful to the EPSRC, UK (grants EP/K005758/1 and EP/M002608/1), Royal Society (UK) (grant IE 160014) and the Russian Foundation for Basic Research (grant No. 17-01-00057) for their financial support.

References

[1] K. Shariff, A. Leonard, Vortex rings, Annual Review of Fluid Mechanics 24 (1) (1992) 235–279. doi:10.1146/annurev.fl.24.010192.001315.

[2] D. Akhmetov, Vortex Rings, Springer-Verlag Berlin Heidelberg, 2009. doi:http://dx.doi.org/10.1007/978-3-642-05016-9.

[3] S. Begg, F. B. Kaplanski, S. S. Sazhin, M. Hindle, M. Heikal, Vortex ring-like structures in gasoline fuel sprays under cold-start conditions, International Journal of Engine Research 10 (4) (2009) 195–214. doi:10.1243/14680874JER02809.

[4] J. Ferry, S. Balachandar, A fast eulerian method for disperse two-phase flow, International Journal of Multiphase Flow 27 (7) (2001) 1199 – 1226. doi:10.1016/S0301-9322(00)00069-0.

[5] D. Healy, J. Young, Full lagrangian methods for calculating particle concentration fields in dilute gas-particle flows, Proceedings of the Royal Society of London A: Mathematical, Physical and Engineering Sciences 461 (2059) (2005) 2197–2225. doi:10.1098/rspa.2004.1413.

[6] A. N. Osiptsov, Lagrangian modelling of dust admixture in gas flows, Astrophysics and Space Science 274 (1-2) (2000) 377–386. doi:10.1023/A:1026557603451.

[7] A. Osiptsov, Investigation of regions of unbounded growth of the particle concentration in disperse flows, Fluid Dynamics 19 (3) (1984) 378–385. doi:10.1007/BF01093900.

[8] H. Helmholtz, Lxiii. on integrals of the hydrodynamical equations, which express vortex-motion, Philosophical Magazine Series 4 33 (226) (1867) 485–512. doi:10.1080/14786446708639824.

[9] H. Lamb, Hydrodynamics, Cambridge University Press, 1895.

[10] P. G. Saffman, Vortex Dynamics, Cambridge University Press, 1992.

[11] S. L. Wakelin, N. Riley, On the formation and propagation of vortex rings and pairs of vortex rings, Journal of Fluid Mechanics 332 (1997) 121–139.

[12] M. Gharib, E. Rambod, K. Shariff, A universal time scale for vortex ring formation, Journal of Fluid Mechanics 360 (1998) 121–140. doi:10.1017/S0022112097008410.

[13] I. Danaila, F. B. Kaplanski, S. S. Sazhin, Modelling of confined vortex rings, Journal of Fluid Mechanics 774 (2015) 267–297. doi:10.1017/jfm.2015.261.

[14] I. Danaila, F. Kaplanski, S. S. Sazhin, A model for confined vortex rings with elliptical-core vorticity distribution, Journal of Fluid Mechanics 811 (2017) 67–94. doi:10.1017/jfm.2016.752.

[15] A. Kaltaev, Application of integral transformation method to concentrated vortice investigation, Ph.D. thesis, Kazakh State University, Almaty, (in Russian) (1983).

[16] F. B. Kaplanski, S. S. Sazhin, Y. Fukumoto, S. Begg, M. Heikal, A generalized vortex ring model, Journal of Fluid Mechanics 622 (2009) 233–258. doi:10.1017/S0022112008005168.

[17] Y. Fukumoto, Global time evolution of viscous vortex rings, Theoretical and Computational Fluid Dynamics 24 (1-4) (2010) 335–347. doi:10.1007/s00162-009-0155-0.

[18] F. B. Kaplanski, S. S. Sazhin, Y. Rudi, Particle dynamics and mixing in an oscillating viscous vortex pair, Proceedings of the Estonian Academy of Sciences Engineering 11 (2) (2005) 140–153.

[19] F. B. Kaplanski, Y. A. Rudi, A model for the formation of "optimal" vortex rings taking into account viscosity, Physics of Fluids 17 (8) (2005) 087101–1 – 087101–7. doi:http://dx.doi.org/10.1063/1.1996928.

[20] N. A. Lebedeva, A. N. Osiptsov, S. S. Sazhin, A combined fully Lagrangian approach to mesh-free modelling of transient two-phase flows, Atomization and Sprays 23 (1) (2013) 47–69. doi:10.1615/AtomizSpr.2013006269.

[21] T. S. Yang, S. S. Shy, Two-way interaction between solid particles and homogeneous air turbulence: particle settling rate and turbulence modification measurements, Journal of Fluid Mechanics 526 (2005) 171–216. doi:10.1017/S0022112004002861.

[22] K. D. Squires, J. K. Eaton, Preferential concentration of particles by turbulence, Physics of Fluids A: Fluid Dynamics (1989-1993) 3 (5) (1991) 1169–1178. doi:http://dx.doi.org/10.1063/1.858045.

[23] S. Goto, J. C. Vassilicos, Self-similar clustering of inertial particles and zero-acceleration points in fully developed two-dimensional turbulence, Physics of Fluids 18 (11). doi:http://dx.doi.org/10.1063/1.2364263.

[24] L. Chen, S. Goto, J. C. Vassilicos, Turbulent clustering of stagnation points and inertial particles, Journal of Fluid Mechanics 553 (2006) 143–154. doi:10.1017/S0022112006009177.

[25] A. Soldati, C. Marchioli, Physics and modelling of turbulent particle deposition and entrainment: Review of a systematic study, International Journal of Multiphase Flow 35 (9) (2009) 827 – 839, special Issue: Point-Particle Model for Disperse Turbulent Flows. doi:http://dx.doi.org/10.1016/j.ijmultiphaseflow.2009.02.016.

[26] K. Domon, O. Ishihara, S. Watanabe, Mass transport by a vortex ring, Journal of the Physical Society of Japan 69 (1) (2000) 120–123. doi:10.1143/JPSJ.69.120.

[27] M. R. Foster, P. W. Duck, R. E. Hewitt, The unsteady krmn problem for a dilute particle suspension, Journal of Fluid Mechanics 474 (2003) 379–409. doi:10.1017/S0022112002002690.

[28] N. Lebedeva, A. Osiptsov, Structure of inertial-admixture accumulation zones in a tornado-like flow, Fluid Dynamics 44 (1) (2009) 68–79. doi:10.1134/S0015462809010074.

[29] F. E. Marble, Dynamics of dusty gases, Annual Review of Fluid Mechanics 2 (1970) 397–446. doi:10.1146/annurev.fl.02.010170.002145.

[30] V. M. Voloshchuk, Introduction to the Hydrodynamics of Coarsely Dispersed Aerosols, Gidrometeoizdat, 1971, (in Russian).

[31] S. A. Ershin, Hydrodynamics, Kazakh University, Almaty, 2013, (in Russian).

[32] F. B. Kaplanski, S. S. Sazhin, S. Begg, Y. Fukumoto, M. Heikal, Dynamics of vortex rings and spray-induced vortex ring-like structures, European Journal of Mechanics - B/Fluids 29 (3) (2010) 208 – 216. doi:http://dx.doi.org/10.1016/j.euromechflu.2010.01.002.

[33] F. B. Kaplanski, U. Rudi, Dynamics of a viscous vortex ring, International Journal of Fluid Mechanics Research 26 (5-6) (1999) 618–630.

[34] I. Danaila, J. Hélie, Numerical simulation of the postformation evolution of a laminar vortex ring, Physics of Fluids 20 (7). doi:10.1063/1.2949286.

[35] Y. Fukumoto, F. B. Kaplanski, Global time evolution of an axisymmetric vortex ring at low Reynolds numbers, Physics of Fluids 20 (5). doi:10.1063/1.2925682.

[36] Boost C++ Libraries, Boost 1.53.0 library documentation-Http://www.boost.org/users/history/version_1_53_0.html. Accessed: 26.10.2014.

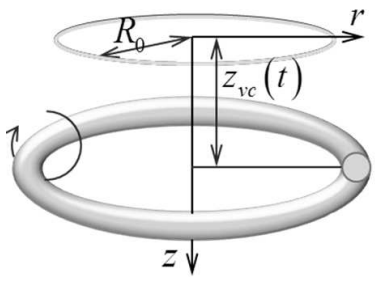

Figure 1: Flow diagram of the vortex ring.

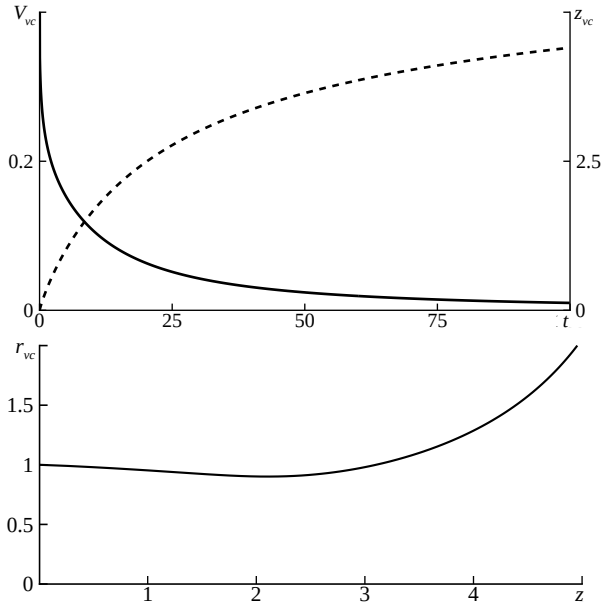

Figure 2: Vortex centroid axial velocity (solid curve) and position in the axial direction (dashed curve) versus time, (top); Vortex centroid position in the radial direction (bottom) versus z; Re = 100.

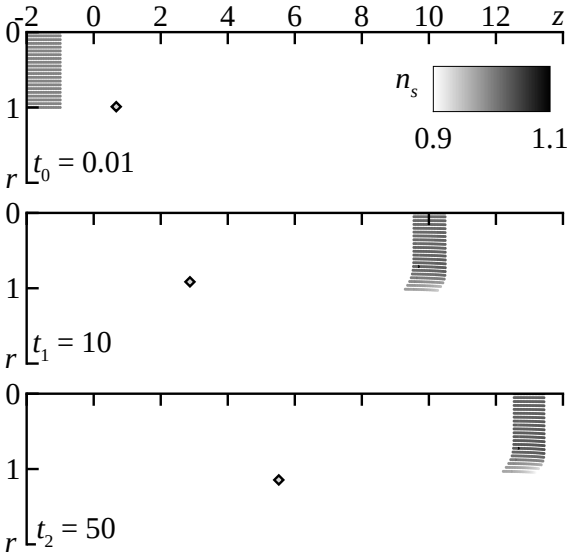

Figure 3: Evolution of the cloud of particles and their number concentration; positions of the vortex centroid (diamond); Re = 100, Stk = 8; $t = t_0 = 0.01$, $t = 10$, $t = 50$.

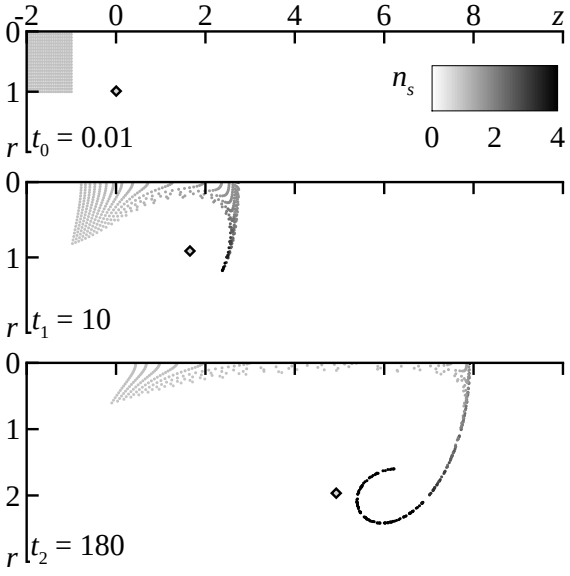

Figure 4: Evolution of the cloud of particles and their number concentration; positions of the vortex centroid (diamond); Re = 100, Stk = 0.32; $t = t_0 = 0.01$, $t = 10$, $t = 180$.

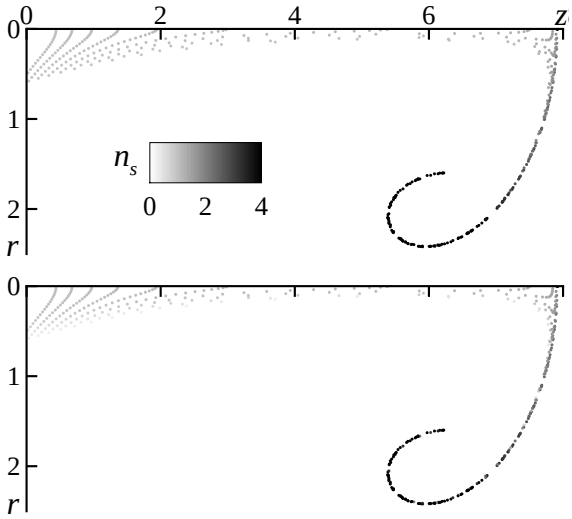

Figure 5: Admixture number density distribution for uniform (top) and non-uniform (bottom) initial number densities; Re = 100, Stk = 0.32; $t = 180$. For the non-uniform distribution, the number density was higher near the axis.

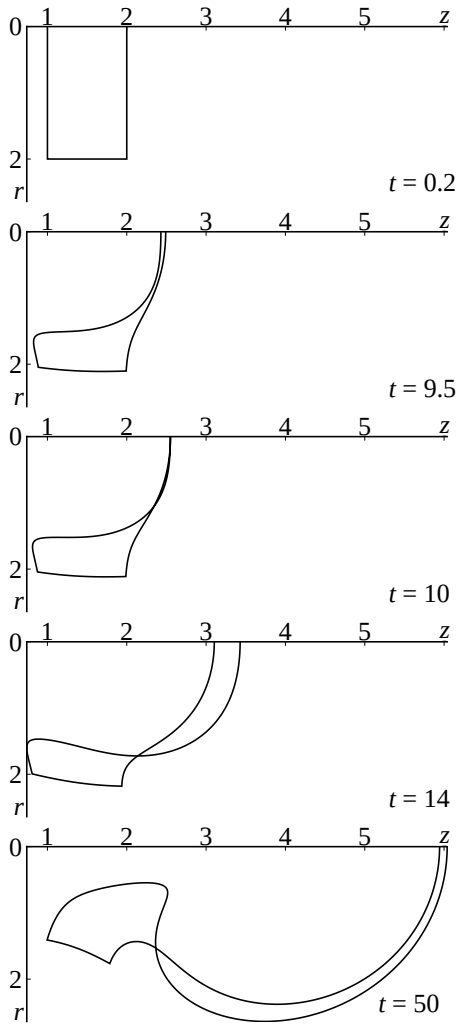

Figure 6: Evolution of a Lagrangian frame of the cloud of particles in interaction with the vortex ring; Re = 100, Stk = 8; $t = t_0 = 0.2$, $t = 9.5$, $t = 10$, $t = 14$, $t = 50$.

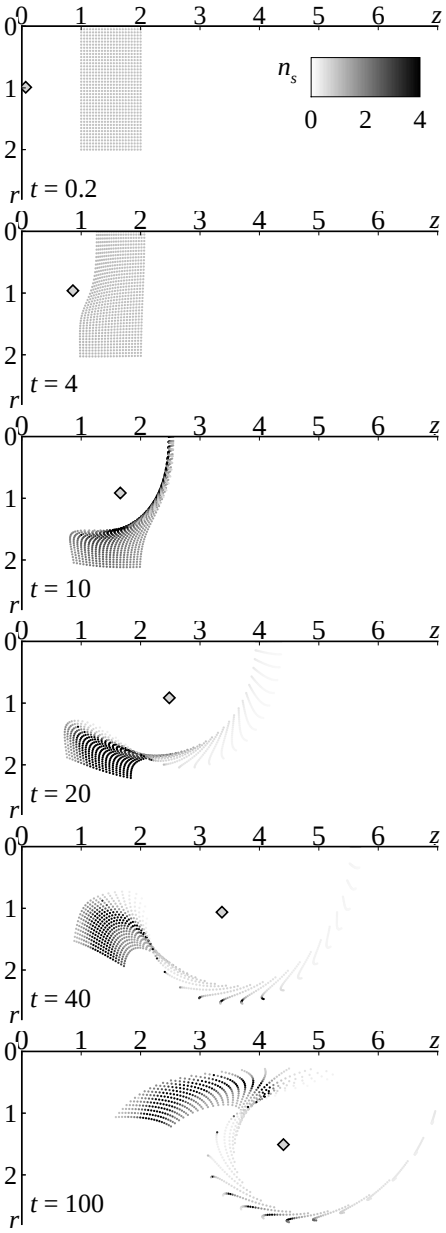

Figure 7: Evolution of the cloud of particles and their number concentration; positions of the vortex centroid (diamond); Re = 100, Stk = 8.

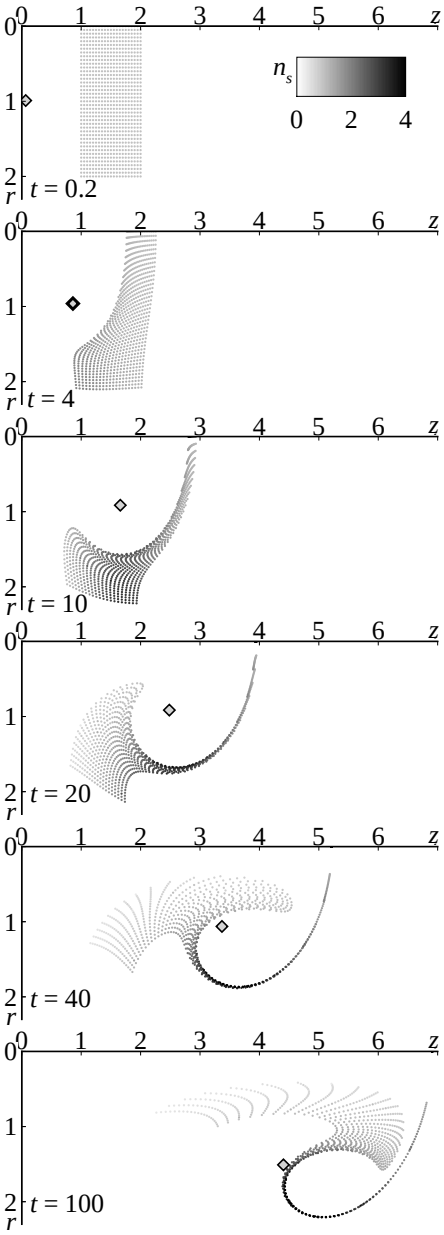

Figure 8: Evolution of the cloud of particles and their number concentration; positions of the vortex centroid (diamond); Re = 100, Stk = 0.32.